Durability of seawater and sea sand concrete (SWSSC) and SWSSC-filled FRP/stainless steel tubular stub columns

Ying-Lei Li[1], Xiao-Ling Zhao[1*] and R.K. Singh Raman[2,3]

[1]School of Civil and Environmental Engineering, UNSW Sydney, Kensington, NSW, Australia

(*corresponding author: xiaolin.zhao@unsw.edu.au)

[2]Department of Mechanical and Aerospace Engineering, Monash University, Clayton, Victoria, Australia

[3]Department of Chemical Engineering, Monash University, Clayton, Victoria, Australia

Abstract

This paper presents an experimental investigation on the durability behaviour of seawater sea sand concrete (SWSSC) and SWSSC-filled FRP/stainless steel tubular stub columns. Effects of NaCl of seawater on the strength of SWSSC, and on the deterioration of FRP were studied. Accelerated degradation tests were conducted on FRP rings exposed to a combined environment of 3.5% NaCl solution and SWSSC. Obvious hoop strength reductions were observed in glass (G)-FRP and basalt (B)-FRP rings after 6-month exposure at 60 °C. SWSSC-filled GFRP tubular stub columns were exposed to an in-door environment (i.e., aged in air at room temperature) for a maximum duration of 2.5 years and no degradation was found by comparing the axial compressive test results from unexposed and exposed specimens. SWSSC-filled stainless steel tubes did not show any deterioration in strength after a 2.5-year exposure to an in-door environment or a 1.5-year immersion in NaCl solution. This study indicated that a hydrothermal environment (e.g., full immersion in solution) is much more aggressive to FRP than a dry environment. The reliability of using accelerated degradation test data to estimate the long-term performance of FRP-related structures in a real environment may need further research.

Keywords:

Durability; Seawater and sea sand concrete (SWSSC); Fibre reinforced polymer (FRP); Hybrid sections; Compressive test

1. Introduction

Utilizing seawater and un-washed sea sand is a promising way in concrete industry to achieve environmental and economic benefits by avoiding the consumption of freshwater and river sand. However, the chloride ions in sea water and sea sand concrete (SWSSC) cause noticeable corrosion on steel reinforcements (Shalon and Rapheal, 1959). Various techniques have been proposed to resolve this corrosion issue, including the use of corrosion inhibitors, coating, electrochemical techniques and replacing carbon steel by corrosion resistant materials such as stainless steel and fibre reinforced polymer (FRP) (Goyal et al., 2018). The concept of hybrid sections consisting SWSSC, FRP and/or stainless steel were proposed for new constructions in recent years (Chen et al., 2020; Teng et al., 2011; Li et al., 2016; Teng et al., 2019), which is an appropriate structural form for columns as the concrete strength could be greatly enhanced by the confinement effect provided by encasing tubes. The short-term structural behaviour of SWSSC-filled FRP and stainless steel tubes under axial compression has been extensively studied and the superior structural performance of the hybrid section as compressive members has been widely demonstrated (Li and Zhao, 2020; Chen et al., 2017). Nevertheless, its long-term performance has not been well understood.

Many studies (Katano et al., 2013; Ramaswamy et al., 1982) have observed that a concrete with seawater and/or sea sand exhibited a more rapid compressive strength development during its early age than ordinary concrete. The compressive strength increase could last for 28 days (Islam et al., 2012) to five years (Mohammed et al., 2004). A number of studies have been conducted on the effects of seawater and sea sand on concrete durability, such as chloride penetration (Huiguang et al., 2011), carbonization (Liu et al., 2016), freeze–thaw resistance (Yamato et al., 1987) and drying shrinkage

(Katano et al., 2013). Due to the complexity of concrete, it is still difficult to reach a solid consensus about the effects of seawater and sea sand on concrete properties (Xiao et al., 2017). However, it is generally agreed that the properties of plain concrete (i.e., without any reinforcement) are not significantly affected by seawater or sea sand and the major concern is chloride-related corrosion on steel reinforcements in concrete.

Fibre reinforced polymer (FRP) generally has the features of high corrosion resistance, high strength, low maintenance, anisotropic mechanical properties, transparent to magnetic fields, low elastic modulus, linear-elastic stress-strain response, low ductility and low creep-rupture threshold (Bank, 2006). The durability of FRP has been extensively studied in recent decades and the external factors affecting the long-term behaviour of FRP include moisture, alkali, acid, salt, temperature, stress, fatigue and ultraviolet radiation (GangaRao et al., 2006; Liu et al., 2020; Raman et al., 2020). The deterioration of FRP results from the degradation of matrix, fibre and the fibre-matrix interphase (Nkurunziza et al., 2005). Since excessively long-term tests can be prohibitive, accelerated degradation tests are widely adopted to assess the durability performance of FRP, in which the material deteriorates at a higher rate by using high aging temperatures. Prediction models, mostly derived from Arrhenius law (Litherland et al., 1981) or Fick's law of diffusion (Katsuki and Uomoto, 1995), have been proposed to corelate the short-term accelerated degradation test data to the long-term performance of FRP. On the other hand, stainless steels that exhibit a superior corrosion resistance (Flint and Cox, 1988) have been successfully used to reinforce concrete structures (e.g., Broadmeadow Bridge) subjected to harsh environments (Cochrane, 2003; BA84/02, 2002).

A number of studies have been conducted on the durability of concrete-filled FRP wraps subjected to alkaline/acidic/saltine solutions (Eldridge and Fam, 2014; Kshirsagar et al., 2000; Liu et al., 2002; Micelli and Myers, 2008), ultraviolet radiation, salt fog cycles (Silva, 2007), wet/dry cycles, freeze/thaw cycles (Toutanji and Deng, 2002; Toutanji and Balaguru, 1998), and sustained load

(Wang and ElGawady, 2019). Eldridge and Fam (2014) found that the reduction of strengthening ratio (i.e., confined-to-unconfined concrete strength ratio f_{cc}'/f_c') of bioregion-GFRP wrapped concrete cylinders was about 25% after 300-day immersion in saltine solution and the effect of solution temperature on the degradation was insignificant. Durability of SWSSC-filled FRP tubes in 40 °C saltine solution was investigated by Li et al. (2018b). The averaged reduction of f_{cc}'/f_c' after 6-month exposure was 45%, 28% and 44% for SWSSC-filled glass/carbon/basalt FRP tubes respectively.

Currently, the long-term durability data of FRP or concrete-FRP composites is rather scarce. An 11-year outdoor exposure test on CFRP plates indicated no clear change in the tensile strength along fibre direction and only small reductions occurred in tensile strength perpendicular to fibre direction and in-plane shear strength (Nishizaki et al., 2005). The relaxation levels of FRP cables after 17-year outdoor exposure were investigated in Sasaki and Nishizaki (2012): 10~30% load relaxation was observed for CFRP under preload of $0.8P_u$, 10% reduction was observed for GFRP under $0.25P_u$ preload, and GFRP cables ruptured under $0.4P_u$ preload, where P_u is the ultimate tensile capacity of FRP cables. By examining the microstructure of GFRP bars embedded in concrete for 8 years, Mufti et al. (2007) concluded no degradation. Based on the study of Xie et al. (2018), the strength reduction of CFRP wrapped concrete cylinders subjected to 30-month natural environment exposure was about 10% and most of the reduction occurred within the first 18 months. By comparing the accelerated degradation test data and long-term data, it seems that the accelerated laboratory environment was much harsher than real environments due to unlimited supply of hydroxyl ions and full saturation for conditioned specimens (Mufti et al., 2007).

Although FRP has potential to reinforce SWSSC, confident experimental or field evidence is still missing to demonstrate the superior durability of SWSSC-FRP composites. In the authors' previous study (Li et al., 2018b), noticeable strength reduction was observed for SWSSC-filled FRP tubes

immersed in 40 °C saltine solution for 6 months. However, the natural environment is probably not as severe as the accelerated degradation environment as indicated by the limited field data of FRP (Nishizaki et al., 2005; Sasaki and Nishizaki, 2012; Mufti et al., 2007). The long-term performance prediction by accelerated degradation test data is yet to be amply supported by field test demonstration. It is worthwhile to investigate the long-term behavior of SWSSC-filled FRP/stainless steel tubes subjected to "real" natural environments to promote a reliable application of SWSSC in infrastructure. This paper presents an experimental study on the long-term behaviour of SWSSC-filled FRP/stainless steel tubular stub columns subjected to natural in-door environment up to 2.5 years. In order to understand the mechanism of the capacity change of stub columns, the compressive and tensile strength development of plain SWSSC and the degradation of FRP alone were also investigated.

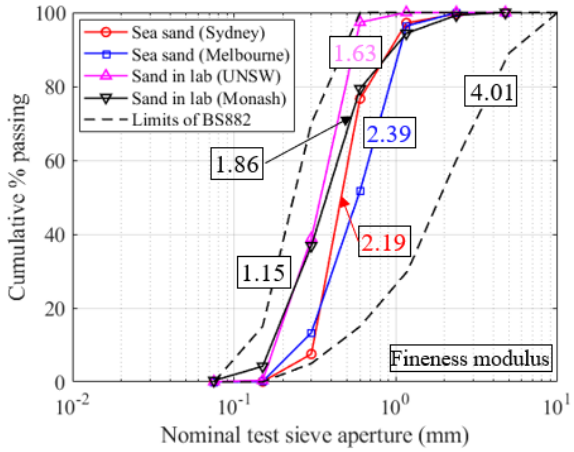

Fig. 1 Particle size distribution curves of sea sand

2. Seawater and sea sand concrete

2.1 Concrete mixtures

Seawater and sea sand concrete (SWSSC) investigated in the present study was made of alkali-activated slag (binder), seawater, sea sand (collected in Brighton beach, Melbourne), coarse aggregate (~14 mm) and hydrated lime slurry to improve workability (Table 1). The activator is sodium meta-silicate in powder form, which contained 46.6% of SiO_2 and 35.8% Na_2O. Chemical compositions of slag, sea sand, seawater and sodium meta-silicate were determined and reported in Li et al. (2018c). Freshwater and river sand concrete (FWRSC) was also prepared and tested in this study and its

composition is shown in Table 1. Before mixing, the solid sodium meta-silicate was preblended with slag in dry state. The mixing procedures for SWSSC and FWRSC were the same.

Table 1 Concrete mixture (kg/m^3).

Constituents	SWSSC	FWRSC
Slag	360	360
Seawater	190	N/A
Freshwater	N/A	190
Sea sand	830	N/A
River sand	N/A	830
Coarse aggregate	1130	1130
Sodium meta-silicate	38.4	38.4
Hydrated lime slurry	14.4	14.4

It is known that the grading of aggregate could somewhat affect the workability and strength of concrete (Mehta and Monteiro, 2006). To guarantee the quality of concrete, standards (BS882, 1992; ASTMC33/C33M, 2018) specify the limits of particle size distribution of aggregates. Fig. 1 shows the particle size distribution curves of sea sand collected in Melbourne and Sydney, normal sand available in laboratories as well as the limits in BS882 (1992). Sand samples obtained from different locations have different particle size distributions but all of them are within the limits. As shown in Fig. 1, a considerably less amount of sea sand could pass through the sieve with 0.3 mm aperture indicating sea sand has fewer fine particles. By calculating the fineness modulus of sand, it is clear that sea sand in this study is coarser than river sand available in the laboratories.

2.2 Mechanical properties

Concrete cylinders (Φ100x200 mm) and prisms (100x100x350 mm) were cast and tested to measure the compressive strength f_c' (AS1012.9:2014, 2014), elastic modulus E_c (AS1012.17-1997(R2014), 2014) by axial compressive test and flexural tensile strength $f_{ct,f}$ (AS1012.11-2000(R2014), 2014)) by four-point bending test respectively. One day after concrete casting, the specimens were demoulded and sealed with plastic films to avoid moisture evaporation. All specimens were stored at room temperature for 28 days. Thereafter, parts of the specimens were tested to get the reference compressive and tensile strength and other specimens were fully immersed in different solutions at

room temperature for durations of 1 month to 1 year. Three identical specimens were tested for each case and the average results were reported in this paper. Four combinations of concrete types and solution types were adopted in this study: SWSSC in freshwater, SWSSC in 3.5% saltwater, FWRSC in 3.5% saltwater and SWSSC in seawater.

Elastic modulus (E_c) is an important parameter in theoretical models for predicting the stress-strain response of FRP-confined concrete. The relationship between E_c and f_c' is presented in Fig. 2 for SWSSC tested in the present study and from existing literature as summarized in Table 2 (Chen et al., 2017; Zeng et al., 2020; Yang et al., 2019), in which SW represents seawater and SS refers sea sand. The E_c- f_c' relationship specified in ACI318-11 (2011) (i.e. $E_c = \sqrt{4730 f_c'}$ in MPa), which applies for normal concrete, is also plotted in Fig. 2. As shown in Fig. 2, almost all points fall within the 20% error of the ACI curve regardless of concrete types or curing regimes. It could be concluded that the E_c- f_c' relationship of SWSSC is similar as that of normal concrete and existing standard (e.g., ACI 318) can be applied for SWSSC to estimate E_c.

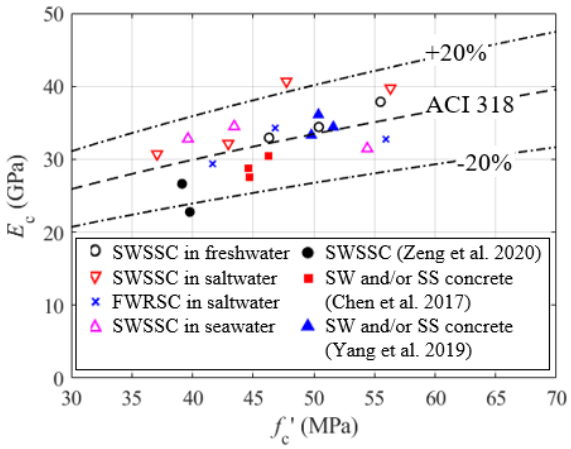

Fig. 2 Relationship between E_c and f_c' of concrete

Table 2 Details of concrete specimens from existing literature.

Data source	Binder	Mixing water	Sand	Curing	Qty[a]	Age
Zeng et al. (2020)	OPC[b]	Seawater or simulated seawater	Sea sand	Laboratory environment	2	More than 35-day
Chen et al. (2017)	OPC	Seawater or freshwater	Sea sand or river sand	Spray with water	3	28-day
Yang et al. (2019)	Alkali-activated slag	Seawater or freshwater	Sea sand or river sand	N/A[c]	3	28-day
Younis et al. (2018)	Slag/OPC=1.85	Seawater	Normal sand	Sea water	1	28, 56-day
Katano et al. (2013)	Slag/OPC=1	Seawater	Sea sand	N/A	3	28, 91-day
Wegian (2010)	OPC	Seawater	Normal sand	Sea water	6	28, 90-day
Xiao et al. (2017)	OPC	Seawater	Sea sand	Sea water	4	28, 90, 180-day
Kaushik and Islam (1995)	OPC	Seawater	Normal sand	Sea water	2	1, 3, 6, 12, 18-month
Ghorab et al. (1989)	OPC or sulphate resisting cement	Seawater	Normal sand	Sea water	2	12, 18-month
Mohammed et al. (2004)	OPC or slag/OPC=0.05~0.7 or fly ash/OPC=0.1~0.2 or slag cement	Seawater	N/A	Sea water	14	1, 5, 10, 15, 20-year

[a]: Quantity of specimen groups.
[b]: OPC=ordinary Portland cement.
[c]: Not given in the literature.

Compressive strength (f_c') and flexural tensile strength ($f_{ct,f}$) of concrete at 28-day and 1-year exposure are presented in Fig. 3 (a), in which the error bar stands for the standard deviation. In generally, the compressive or tensile strength increased by 33% to 56% after 1-year immersion in solutions. SWSSC in saltwater and seawater shows larger compressive strength increase ratio than SWSSC in freshwater and FWRSC in saltwater. It seems that NaCl in concrete and curing water is beneficial to the compressive strength development probably because NaCl improves the pore structure of concrete (Islam et al., 2012). On the other hand, the effect of curing solution type on the flexural tensile strength is not obvious. However, the NaCl in mixing water and aggregate could improve the flexural tensile strength as evidenced by a higher $f_{ct,f}$ of SWSSC than that of FWRSC.

Changes in the compressive strength of seawater and/or sea sand concrete from the present study and existing literature (Kaushik and Islam, 1995; Mohammed et al., 2004; Katano et al., 2013; Younis et al., 2018; Wegian, 2010; Ghorab et al., 1990; Xiao et al., 2017) are plotted in Fig. 3 (b-c), in which the normalized strength is the ratio of compressive strength after exposure to the 28-day compressive strength (i.e., unexposed strength). Details of the concrete specimens are summarized in Table 2 where specimens were exposed to corrosive environment at ambient temperature. As shown in Fig. 3 (b-c), the strength increase could last for three months to five years depending on the concrete mixtures (e.g., binder type, water-to-binder ratio). Study of Mohammed et al. (2004) indicated that slag is helpful to improve the durability but the effect of fly ash is insignificant. Among all the types, concrete with alkali-activated slag as the only binder (specimens prepared in this study) shows the maximum strength increase after 1-year exposure. Except for the specimens in Wegian (2010) and parts of the specimens in Mohammed et al. (2004), the compressive strength after exposure is generally higher than the 28-day compressive strength. For concrete-filled FRP/stainless steel tubes, the strength degradation of concrete should not be a big issue since the concrete is further protected by the encasing tubes.

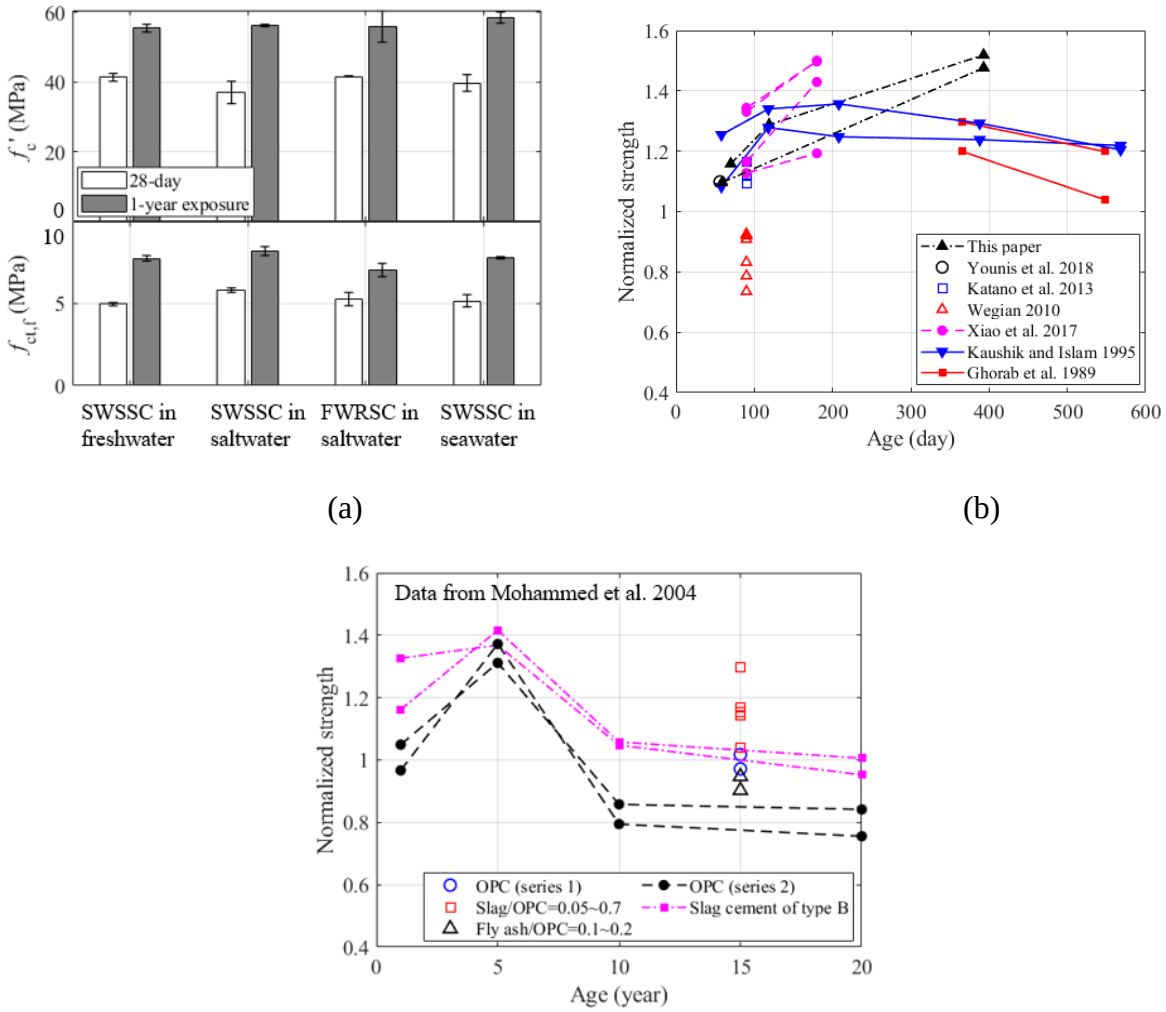

Fig. 3 Strength development of plain concrete in seawater: (a) data of present study; (b) data of literature; (c) data of Mohammed et al. (2004)

3. SWSSC-filled FRP tubular stub columns

3.1 FRP rings in solutions

Three types of filament wound FRP tubes (i.e., E-glass (G)-FRP, carbon (C)-FRP and basalt (B)-FRP) were investigated in this study. Based on manufacturer's data, about 20%, 40% and 40% fibres were oriented in 15°, ±40° and ±75° with respect to the tube axis and the fibre volume ratio is 0.6. FRP fibres in various orientations can provide somewhat longitudinal strength when compared with the case where all the fibres are in the hoop direction. It is not the intention to replace internal longitudinal rebars. The longitudinal strength provided by FRP fibres in various orientations is much less than that achieved by longitudinal rebars. SWSSC-filled double-skin FRP tubes with a length of 250 mm were

first prepared (outer tube: 158x3 mm, inner tube: 100x3 mm) and cured at ambient temperature for 28 days. Then, concrete-filled GFRP and BFRP tubes were cut into 20 mm wide disks by diamond saws. The width for CFRP disks was restricted to 8 mm due to the limited capacity of test apparatus. Aging was conducted by fully immersing these specimens in 3.5% NaCl solution or distilled water in a 5-L capacity beaker (Fig. 4). The beakers were then placed in a commercial-available thermostatic water bath filled with tap water to maintain the target temperature. Three temperatures (room temperature (23 °C), 40 °C and 60 °C) and three immersion durations (30, 90 and 180 days) were chosen to age the specimens. The maximum aging temperature is much lower than the glass transition temperature of polymer matrix of FRP, and it is believed that the degradation mechanisms are the same for these three temperatures. After each period, three specimens were removed from the beakers and the sandwich concrete was removed. Split-disk test in accordance with ASTMD2290-16 (2016) was then conducted on the aged FRP rings to obtain the mechanical properties in hoop direction (same as the test setup in Li et al. (2016)). Unconditioned FRP rings with the same width as conditioned specimens were also tested to get the reference hoop strength.

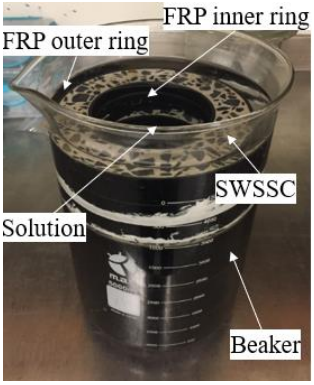

Fig. 4 Immersion of FRP specimens in solution

It is necessary to mention that the alkali ions in concrete could move to the solutions, which leads to an increase of the pH of the solution. The pH of the saltwater, in which the SWSSC-filled double-skin BFRP tubes were immersed, at 1-, 50-, 120- and 180-day are 9.8, 10.1, 11.3 and 12.5 respectively. Due to the influence of concrete, the saltwater and distilled water became alkaline instead of neutral. However, if the specimens are exposed to a real marine environment, the pH of seawater ranges from

7.5 to 8.4, which is less alkaline than the laboratory environment produced in this study. Therefore, this laboratory study may overestimate the degradation of FRP if applied in a real marine environment.

Hoop strength of unexposed FRP outer rings (158x3 mm) is 368.8 MPa, 548.0 MPa and 328.9 MPa for GFRP, CFRP and BFRP respectively, whereas the hoop strength of the inner rings (100x3 mm) is 321.3 MPa, 442.3 MPa and 319.6 MPa respectively. Hoop strength retentions of aged FRP rings (i.e., the ratio of the hoop strength of the aged FRP rings to that of the unconditioned FRP rings) are summarized in Fig. 5. In general, the strength of FRP decreases with the increase of aging temperature and aging time. The degradation process of FRP tends to slow down with the increase of aging time. No obvious difference is observed in terms of the hoop strength retention of the inner and outer rings. Therefore, the environment combinations do not affect the durability of FRP and the same design theory can be applied to both outer and inner tubes of SWSSC-filled double-skin tubular columns. Based on the strength retention data of GFRP and BFRP at 60 °C, distilled water is slightly more aggressive than saltwater. It is probably because the NaCl in saltwater could block the pathway of water molecular movement in FRP to slow down the diffusion process. It can be concluded that NaCl in SWSSC or seawater does not worsen the durability behaviour of FRP and it even has some beneficial effects. Fig. 5 shows that CFRP has much superior durability than GFRP or BFRP, which agrees with past studies (Wang et al., 2017). BFRP behaves similar to GFRP at 60 °C, but a greater strength loss is observed for BFRP at 23 and 40 °C indicating BFRP performs worst among the three FRP types.

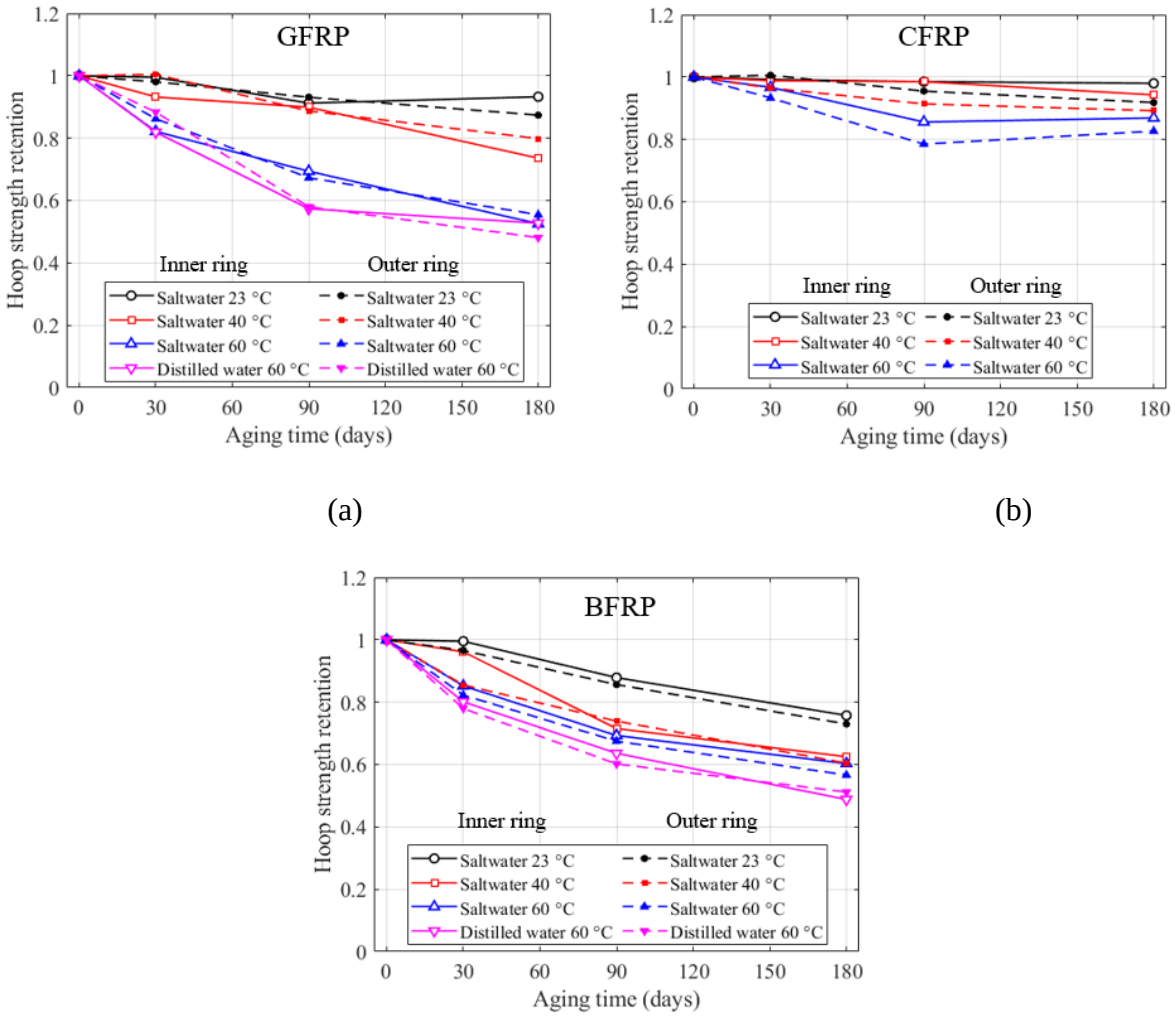

Fig. 5 Hoop strength degradation of FRP rings: (a) GFRP; (b) CFRP; (c) BFRP

3.2 Stub columns in solutions

In the authors' previous paper (Li et al., 2018b), strength reduction of SWSSC-filled G/C/BFRP tubular columns subjected to 3.5% NaCl solution at 40 °C was investigated. After 6 months of exposure, the average hoop strength reduction for columns, which was derived from compressive capacity, reached 35% and 54% for SWSSC-filled GFRP and BFRP columns respectively and the reduction of SWSSC-filled CFRP columns was insignificant. It was found that the hoop strength reduction in columns was faster than that in FRP materials. SWSSC-filled GFRP and BFRP columns did not exhibit a superior durability as expected probably due to the high aging temperature (i.e., 40 °C) and full saturation of specimens.

3.3 Stub columns in air

This section investigates the long-term behaviour of SWSSC-filled GFRP stub columns exposed to an in-door environment for 1 and 2.5 years. After casting concrete, the stub columns were stored in a dry condition in the laboratory at the room temperature. Mixture of SWSSC was listed in Table 1 and the properties of GFRP tube were the same as those reported in Li et al. (2016) with hoop strength as 308.8 MPa and elastic modulus as 25.2 GPa. Axial compressive test was conducted on the stub columns after aging and the experimental setup was described in Li et al. (2016).

A total of 16 specimens, including SWSSC fully filled GFRP tubes and SWSSC filled double-skin tubes (stainless steel as inner and GFRP as outer tubes), were tested in this study. Dimensions of GFRP and stainless steel tubes used in this study are listed in Table 3, where D is outer diameter and t is thickness. Hoop strength of unexposed GFRP (f_{uh}) and yield stress of unexposed stainless steel (f_{ys}) were obtained by disk-split test and tensile coupon test respectively and their values are also listed in Table 3 (Li et al., 2016). Key test results of stub columns are presented in Table 4, where f_c' is unconfined concrete strength at test date and N_t is experimental ultimate load-carrying capacity. The results of unexposed specimens (Li et al., 2016) and specimens immersed in 3.5% NaCl solution (Li et al., 2018b) are also given in Table 4 for a comparison purpose. The label of specimen consists of outer tube name, inner tube name (for double-skin tubes), concrete indicator ("C") and exposure time in month ("0" stands for unexposed specimen).

Table 3 Dimensions and properties of GFRP and stainless steel.

Tube name	D (mm)	t (mm)	f_{uh}[a] or f_{ys}[b] (MPa)	Material type
G50	51	3.07	308.8	GFRP
G101	100	3.13	308.8	GFRP
G114	115	3.13	308.8	GFRP
G165	158	3.14	308.8	GFRP
S50	48	2.82	306.8	Stainless steel
S101	102	2.79	324.4	Stainless steel
S114	114	2.79	270.3	Stainless steel
S165	168	3.22	280.1	Stainless steel

[a]: f_{uh} = hoop strength of FRP.
[b]: f_{ys} = yield stress (i.e., 0.2% proof stress) of stainless steel

Table 4 Specimen table for SWSSC-filled GFRP tubes.

Cross-section	Unexposed[a]			12-month in air			30-month in air			6-month in 40 °C saltwater[b]		
	Specimen	f_c' (MPa)	N_t (kN)	Specimen	f_c' (MPa)	N_t (kN)	Specimen	f_c' (MPa)	N_t (kN)	Specimen	f_c' (MPa)	N_t (kN)
Fully filled 	G50-C-0	29.8	244	G50-C-12	41.7	272	G50-C-30	42.2	323	G50-C-6	63.9	274
	G101-C-0	29.8	670	G101-C-12	41.7	858	G101-C-30	42.2	878	G101-C-6	63.9	842
	G114-C-0	29.8	814	G114-C-12	41.7	982	G114-C-30	42.2	997	G114-C-6	63.9	842
	G165-C-0	29.8	1338	G165-C-12	41.7	1558	G165-C-30	42.2	1662	G165-C-6	63.9	842
Double-skin 	G114-G50-C-0	32.9	797	G114-G50-C-12	38.2	824	G114-G50-C-30	40.2	926	G114-G50-C-6	60.0	870
	G165-G101-C-0	32.9	882	G165-G101-C-12	38.2	1004	G165-G101-C-30	40.2	1015	G165-G101-C-6	60.0	1005
	G114-S50-C-0	32.9	872	G114-S50-C-12	38.2	953	G114-S50-C-30	40.2	1019	G114-S50-C-6	60.0	952
	G165-S101-C-0	32.9	1301	G165-S101-C-12	38.2	1199	G165-S101-C-30	40.2	1223	G165-S101-C-6	60.0	1234

[a]: Adapted from Li et al. (2016).
[b]: Adapted form Li et al. (2018b).

Table 5 Specimen table for SWSSC-filled SS tubes.

Cross-section	Unexposed[a]			12-month in air			30-month in air			18-month in saltwater		
	Specimen	fc' (MPa)	Nt (kN)	Specimen	fc' (MPa)	Nt (kN)	Specimen	fc' (MPa)	Nt (kN)	Specimen	fc' (MPa)	Nt (kN)
Fully filled 	S101-C-0	31.4	729	S101-C-12	41.7	797	S101-C-30	42.2	858	S101-C-18	56.8	915
	S114-C-0	31.4	800	S114-C-12	41.7	926	S114-C-30	42.2	967	S114-C-18	56.8	1055
	S165-C-0	31.4	1522	S165-C-12	41.7	1832	S165-C-30	42.2	1917	S165-C-18	56.8	2161

[a]: Adapted from Li et al. (2016).

Both unexposed and exposed specimens failed by the hoop rupture of outer GFRP tubes and the typical failure modes of specimen group G165-C with and without aging are shown in Fig. 6. After a certain time of aging, the colour of GFRP tube changed from green to slight brown. As shown in Fig. 6, colour change of specimens in air is slight but it is more significant for stub columns in solutions due to a higher deterioration of GFRP tube. Load-axial strain curves of fully filled and double-skin tubes are plotted in Fig. 7 and Fig. 8 respectively, where axial strain is the end shortening divided by column height and the unconfined concrete capacity is equal to unconfined concrete strength multiplied by concrete area. During a loading process, buckling of GFRP tube in longitudinal direction occurred for multiple times accompanied with a slight load drop. The amplitude of load drop for exposed columns is generally lower than that of unexposed columns probably due to a better bonding between GFRP tube and SWSSC for columns with longer curing time. Shapes of load-axial strain curves of unexposed and exposed columns are similar except for specimen G114-C-6 and G165-C-6. Strain hardening of these two specimens were insignificant as the hoop strength of GFRP was greatly degraded due to the harsh environment (i.e., 40 °C saltwater). The capacity of columns aged in air (i.e., exposed to in-door environment) is higher than that of unexposed columns due to their higher concrete strength. Aging time (12 months vs. 30 months) does not obviously affect the load-axial strain curves of aged specimens, which indicates a negligible degradation caused by the in-door environment.

Fig. 6. Typical Failure modes of SWSSC-filled GFRP tubes (G165-C)

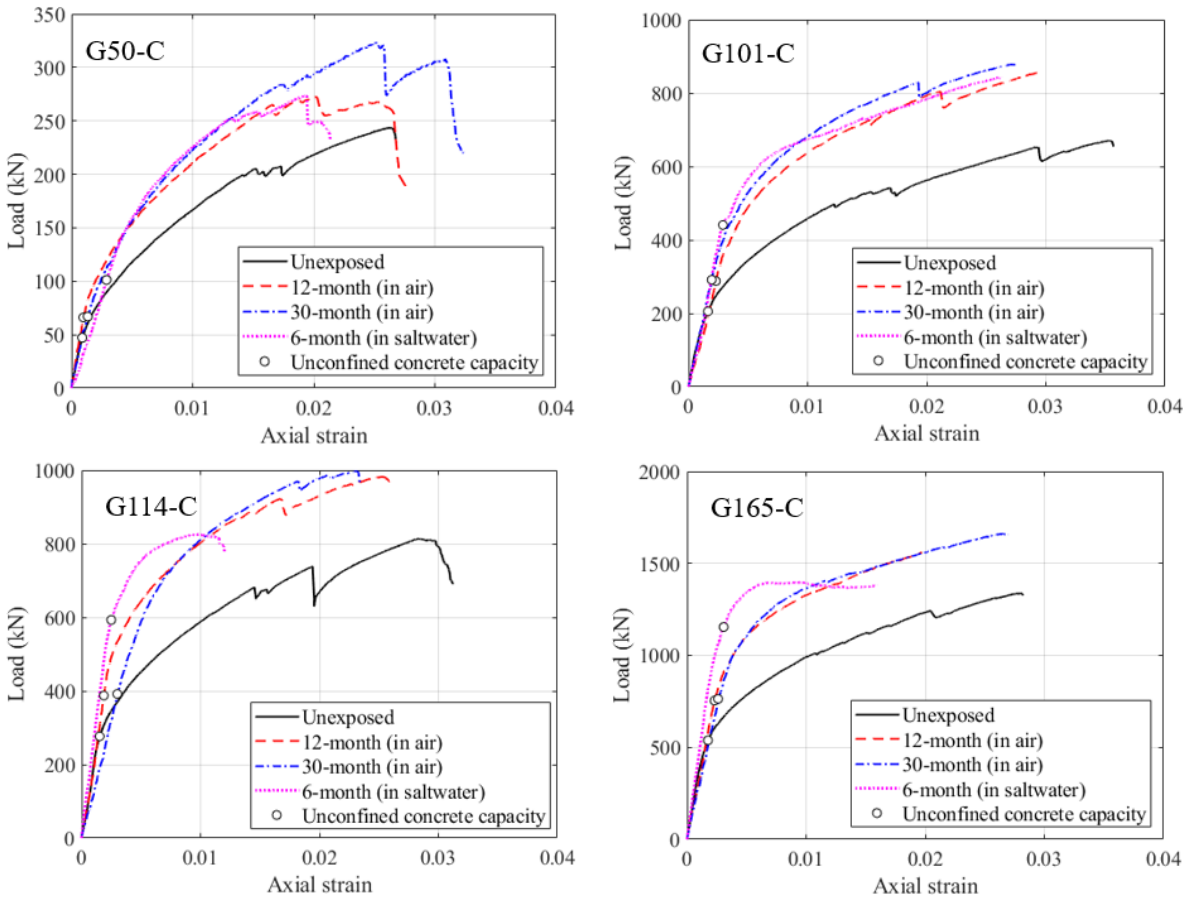

Fig. 7 Load-axial strain curves of SWSSC fully filled GFRP tubes

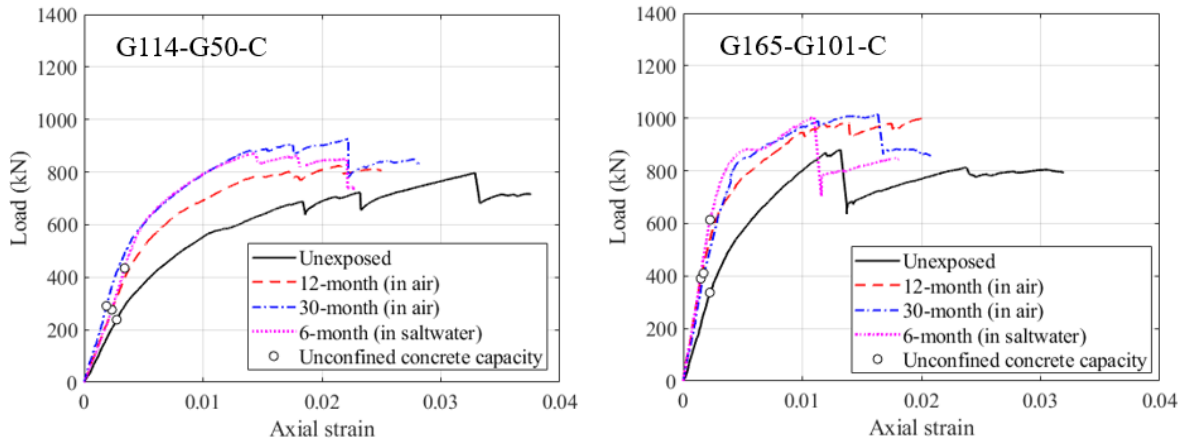

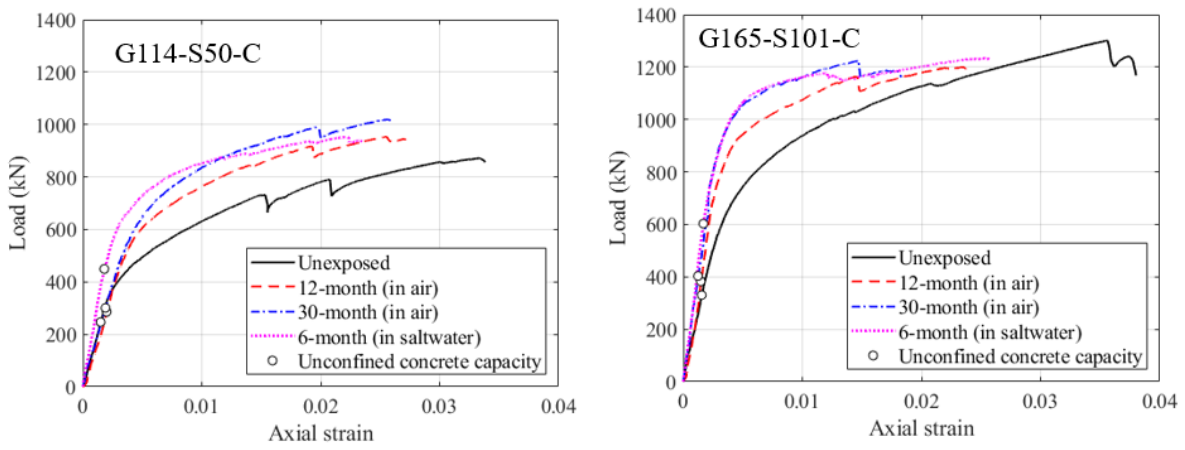

Fig. 8 Load-axial strain curves of SWSSC filled double-skin tubes (GFRP as outer and SS as inner tubes)

As discussed in Section 2.2 and evidenced in Table 4, concrete did not deteriorate and even showed a strength gain within the aging period. In order to exclude the effect of concrete strength change on assessing the durability performance, rupture stress of outer GFRP tube in stub columns (σ_{uh}) was derived from the experimental ultimate capacity (N_t):

$$\sigma_{uh} = \frac{f_l (D_o - 2t_o)}{2t_o} \tag{1}$$

$$f_l = \frac{f'_{cc} - f'_c}{3.5} \tag{2}$$

$$f'_{cc} = \frac{N_t - f_{ys} A_s}{A_c} \tag{3}$$

where f_l is confining pressure, D_o is outer diameter of outer tube, t_o is thickness of outer tube, f_{cc}' is confined concrete strength, f_c' is unconfined concrete strength, A_c is concrete area, f_{ys} is yield stress of stainless steel and A_s is area of stainless steel tube. Eq. (2) is a commonly used equation to specify the strength enhancement of concrete due to confining pressure provided by FRP wrap/tube (Teng et al., 2007; Li et al., 2018a). Eq (3) is based on the assumption that at ultimate condition, load carried by GFRP tube is negligible and load resisted by stainless steel tube is its yield capacity. If there is no stainless steel tube in columns, the term $f_{ys}A_s$ in Eq (3) is zero.

σ_{uh} of stub columns and the exposed-to-unexposed ratio of σ_{uh} are presented in Fig. 9, where each marker in the upper graph represents a specimen and the bar value in the lower graph is an average ratio of a group of specimens. As shown in Fig. 9, specimens aged in air do not show any reduction of rupture stress indicating that no degradation occurred in stub columns. There is even a slight increase of σ_{uh} of aged specimens, which is likely caused by a further curing process of GFRP. However, obvious degradation is found for specimens exposed to 40 °C saltwater water (Li et al., 2018b). It is clear that a wet (hydrothermal) environment is much more aggressive than a dry environment.

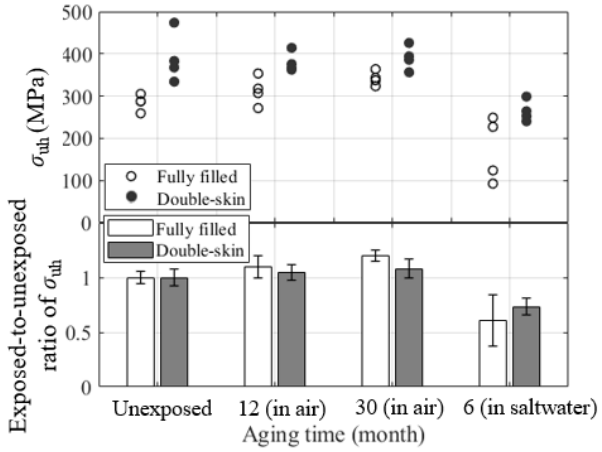

Fig. 9 Ultimate hoop stress of SWSSC-filled GFRP tubes

Based on the accelerated degradation test data in Section 3.1, hoop strength of GFRP at room temperature could be predicted by Arrhenius law (Litherland et al., 1981). Following the procedures documented in Bank et al. (2003), strength retention of GFRP at 23 °C could be estimated by:

$$Y = -24.8\lg(t_{aging}) + 142.8 \quad (4)$$

where Y is strength retention in percentage and t_{aging} is aging time in day. After 2.5 years of aging, the predicted strength reduction of GFRP is 30.6%. However, as shown in Fig. 9, no degradation was observed from experimental results. It seems that the existing degradation model is too conservative when predicting the actual long-term performance of FRP in a dry environment. The unreliability is mainly caused by two reasons: (a) current prediction models have not been validated on the basis of demonstrations from field test data and (b) accelerated degradation test generally uses a solution

environment for an easy control of temperatures but it cannot represent the real environment that FRP is subjected to (e.g., aging in air in this study). Therefore, more studies are needed in this research field to reasonably assess the long-term performance of FRP-related structures.

Besides rupture stress, another indicator of the durability of concrete-filled FRP tubes is strengthening ratio (f_{cc}'/f_c'). The exposed-to-unexposed ratio of f_{cc}'/f_c' was 0.85 and 0.90 for fully filled and double-skin columns aged in air for 1 year, whereas the ratio was 0.90 and 0.87 when they were aged in air for 2.5 years. There is an obvious reduction of strengthening ratios, which seems contradictory to the observed trend of rupture stresses (Fig. 9). It is because of the fact that a significant increase of f_c' of aged concrete could lead to a decrease of f_{cc}'/f_c' although hoop strength of FRP does not degrade (see Eqs (1-2)). Therefore, when using strengthening ratio to assess the durability of concrete-filled FRP tubes, the influence of unconfined concrete strength should be carefully examined. Otherwise, the conclusion drawn from f_{cc}'/f_c' may not be correct.

4. SWSSC-filled stainless steel tubular stub columns

4.1 Stainless steel coupons in solutions

In order to assess the durability of stainless steel (AISI 316 grade in this study), tensile coupon tests were conducted on unexposed and exposed stainless steel coupons cut for tube S165. Edges and surfaces of coupons were not treated such as polishing or sealing. Exposed coupons were fully immersed in 3.5% NaCl solution at temperatures of 23, 40 and 60 °C for durations of 1, 3 and 6 months. After exposure, surface of coupons did not show any changes. As expected, no change of strength (i.e., yield stress and ultimate strength) was observed for all the stainless steel coupons.

4.2 Stub columns in air and solutions

Three groups of SWSSC fully filled stainless steel tubular stub columns, which were aged in air for 12 and 30 months, and in 3.5% NaCl solution for 18 months (6 months at 40 °C and followed by 12

months at 23 °C) respectively, were studied for their durability. Details of the specimens are listed in Table 5, in which f_c' is unconfined concrete strength at test date and N_t is experimental ultimate capacity (defined as the maximum load within 0.05 axial strain). Dimensions of stainless steel tube and its yield stress (without exposure) are reported in Table 3. After each duration, axial compressive test was carried out and the test setup is same as that for SWSSC-filled GFRP tubes.

SWSSC-filled stainless steel tubes before and after aging are shown in Fig. 10 and the stainless steel tube surface did not change obviously after exposure in air or solutions. Failure modes of the unexposed and exposed stub columns are the same. Load-axial strain curves of the stub columns are plotted in Fig. 11 including both unexposed and exposed specimens. Exposed specimens sustained a higher load than unexposed specimens due to the increase of unconfined concrete strength after aging. An obvious descending branch of load-axial strain curves is observed for columns in saltwater and it is also caused by the higher f_c' of 56.8 MPa. Based on previous studies (Li et al., 2019), concrete-filled stainless steel tubes with higher concrete strength or lower confining pressure exhibited a more distinct descending post-peak curve.

Fig. 10. Typical failure modes of SWSSC-filled stainless steel tubes (S165-C)

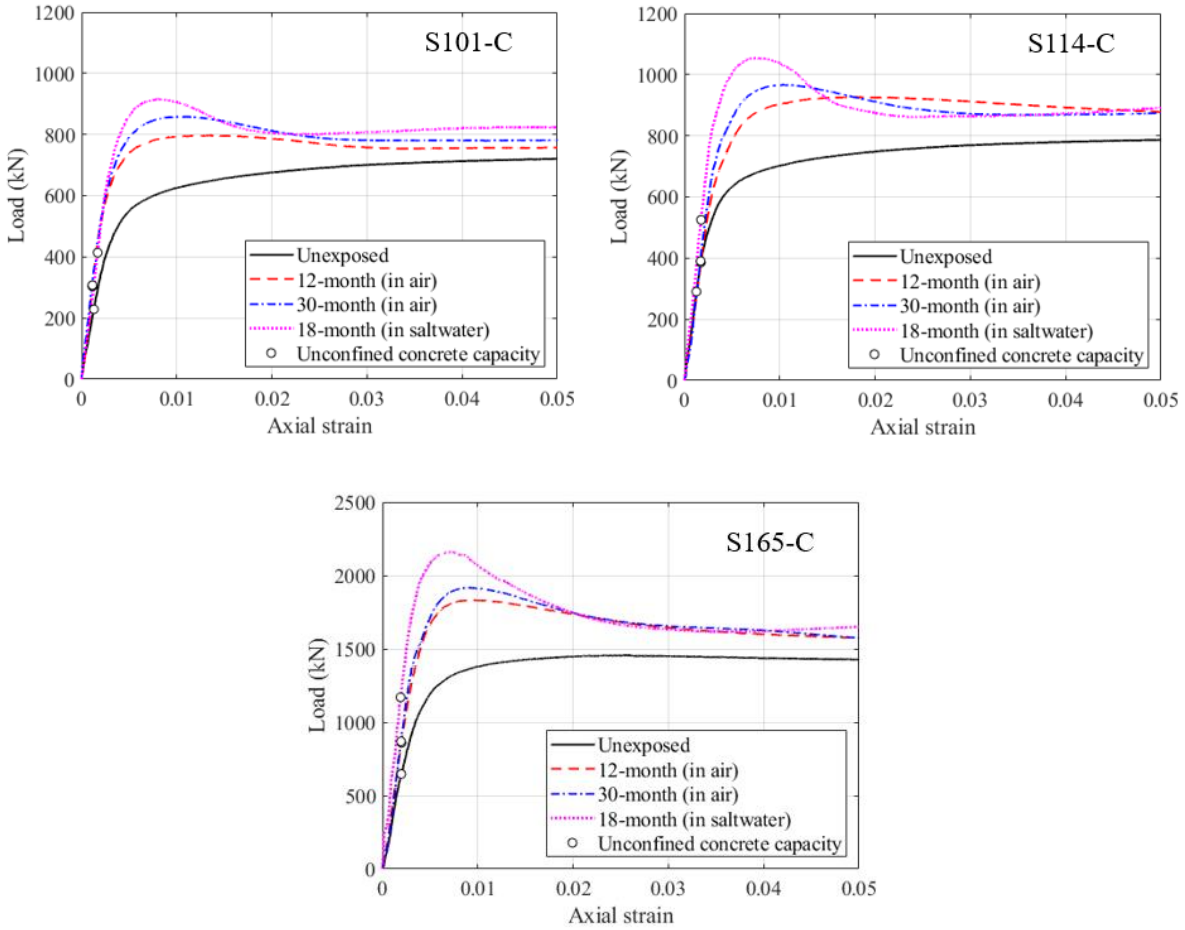

Fig. 11 Load-axial strain curves of SWSSC fully filled SS tubes

Due to the strength development of concrete, effect of environments on the durability behavior of SWSSC-filled stainless steel columns cannot be cleared identified from the load-axial strain curves. Yield stress of stainless steel tube, which is derived from the ultimate capacity, is selected as the durability indicator for stub columns. In Li et al. (2018d), the ultimate compressive capacity of concrete-filled SS tubes can be estimated by:

$$N_{\mathrm{u}} = (A_{\mathrm{c}} + A_{\mathrm{s}})\, f_{\mathrm{scy}} \tag{5}$$

$$f_{\mathrm{scy}} = (1 + 1.41\xi)\, f_{\mathrm{c}}' \tag{6}$$

$$\xi = \frac{f_{\mathrm{ys}} A_{\mathrm{o}}}{f_{\mathrm{c}}' A_{\mathrm{c}}} \tag{7}$$

where N_{u} is predicted ultimate capacity, A_{c} is concrete area, A_{s} is stainless steel tube area, f_{scy} is nominal yield strength of composite section, ξ is confinement factor, f_{ys} is yield stress of stainless steel, f_{c}' is unconfined concrete strength. If N_{u} is set as experimental capacity N_{t}, yield stress of

stainless steel tube in a column could be "back calculated". This yield stress is denoted as σ_y to highlight that f_{ys} is an intrinsic property of stainless steel but σ_y is the derived yield stress in stainless steel tube at the ultimate condition of a column. σ_y of unexposed and exposed columns and the averaged exposed-to-unexposed ratio of σ_y are presented in Fig. 12. Stub column dose not degrade after exposure as evidenced by the bar graph of exposed-to-unexposed ratio of σ_y in Fig. 12. It can be concluded that SWSSC-filled stainless steel tubes does not deteriorate after 30-month aging in air or 18-month aging in saltwater.

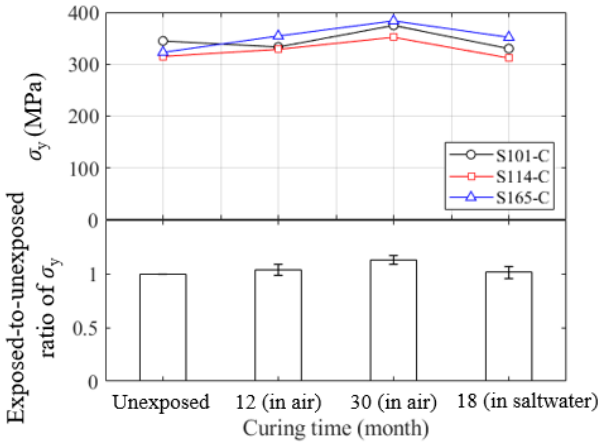

Fig. 12. Yield stress of SWSSC fully filled SS tubes

5. Conclusions

The study presented herein intended to investigate the effects of aging on the mechanical properties of SWSSC and SWSSC-filled FRP/stainless steel tubular stub columns. The following conclusions could be drawn:

(1) Sodium chloride in SWSSC and curing water was beneficial for the strength development of plain concrete (i.e. without any reinforcement). Relationship between elastic modulus and concrete strength of normal concrete (e.g., ACI 318) could be applied for SWSSC.

(2) Durability of FRP in terms of hoop strength followed the order of CFRP>GFRP>BFRP. Environment combination with inner SWSSC and outer solution affected the durability of FRP to the

same extent as the combination with inner solution and outer SWSSC. As compared to distilled water, NaCl in seawater does not worsen the durability of FRP.

(3) SWSSC-filled GFRP tubes did not show obvious strength degradation after 2.5 years of aging in air. A wet (hydrothermal) environment is much more aggressive for FRP than a dry environment. The existing degradation model was too conservative when it was used to predict the long-term performance of FRP in a dry environment.

(4) After 2.5-year aging in air or 1.5-year exposure to saltwater, SWSSC-filled stainless steel tubes exhibited no capacity reduction.

Acknowledgement

Financial support provided by ARC Discovery Grant (DP160100739) from the Australian Research Council (ARC) is greatly appreciated. The authors thank the support from Bayside City Council for collection of sea sand and seawater. Laboratory staffs, Mr. Long Goh, Mr. Saravanan Mani and Mr. Jeff Doddrell, at Monash University is also acknowledged for their assistance.

References

ACI 318-11 (2011) Building code requirements for structural concrete and commentary.

AS 1012.9:2014 (2014) Methods of testing concrete - Compressive strength tests - Concrete, mortar and grout specimens.

AS 1012.11-2000 (R2014) (2014) Methods of testing concrete - Determination of the modulus of rupture.

AS 1012.17-1997 (R2014) (2014) Methods of testing concrete - Determination of the static chord modulus of elasticity and Poisson's ratio of concrete specimens.

ASTM C33/C33M (2018) Standard specification for concrete aggregates.

ASTM D2290-16 (2016) Standard Test Method for Apparent Hoop Tensile Strength of Plastic or Reinforced Plastic Pipe.

BA 84/02 (2002) Use of Stainless Steel Reinforcement in Highway Structures, The Highways Agency.

Bank LC (2006) *Composites for construction: Structural design with FRP materials.* Hoboken, New Jersey: John Wiley & Sons.

Bank LC, Gentry TR, Thompson BP, et al. (2003) A model specification for FRP composites for civil engineering structures. *Construction and Building Materials* 17: 405-437.

BS 882 (1992) Specification for aggregates from natural sources for concrete, British Standards Institution.

Chen GM, He ZB, Jiang T, et al. (2017) Axial compression tests on FRP-confined seawater/sea-sand concrete. In: *6th Asia-Pacific Conference on FRP in Structures*.

Chen GM, Liu PC and Chen JF (2020) Compressive behaviour of sea sand filled CFRP tubular columns. In: *Third International Workshop on Seawater Sea-Sand Concrete (SSC) Structures Reinforced with FRP Composites* (eds Teng JG, Chen JF, Yu T, et al.), Shenzhen, China, pp.43-44.

Cochrane D (2003) Success for stainless steel. *Concrete Journal, March issue*. 26-28.

Eldridge A and Fam A (2014) Durability of concrete cylinders wrapped with gfrp made from furfuryl alcohol bioresin. *Journal of Composites for Construction* 18(6): 04014013.
Flint G and Cox R (1988) The resistance of stainless steel partly embedded in concrete to corrosion by seawater. *Magazine of Concrete Research* 40(142): 13-27.
GangaRao HV, Taly N and Vijay P (2006) *Reinforced concrete design with FRP composites*. CRC press.
Ghorab HY, Hilal M and Antar A (1990) Effect of mixing and curing waters on the behaviour of cement pastes and concrete Part 2: Properties of cement paste and concrete. *Cement and Concrete Research* 20(1): 69-72.
Goyal A, Pouya HS, Ganjian E, et al. (2018) A review of corrosion and protection of steel in concrete. *Arabian Journal for Science and Engineering* 43(10): 5035-5055.
Huiguang Y, Yan L, Quan LH, et al. (2011) Durability of sea-sand containing concrete: Effects of chloride ion penetration. *Mining Science and Technology* 21(1): 123-127.
Islam MM, Islam MS, Al-Amin M, et al. (2012) Suitability of sea water on curing and compressive strength of structural concrete. *Journal of Civil Engineering (IEB)* 40(1): 37-45.
Katano K, Takeda N, Ishizeki Y, et al. (2013) Properties and application of concrete made with sea water and un-washed sea sand. In: *Third International Conference on Sustainable Construction Materials and Technologies*, Kyoto, Japan.
Katsuki F and Uomoto T (1995) Prediction of deterioration of FRP rods due to alkali attack. *Non-Metallic (FRP) Reinforcement for Concrete Structures: Proceedings of the Second International RILEM Symposium*. CRC Press, 82.
Kaushik SK and Islam S (1995) Suitability of sea water for mixing structural concrete exposed to a marine environment. *Cement and Concrete Composites* 17(3): 177-185.
Kshirsagar S, Lopez-Anido RA and Gupta RK (2000) Environmental aging of fiber-reinforced polymer-wrapped concrete cylinders. *Materials Journal* 97(6): 703-712.
Li Y-L and Zhao X-L (2020) Hybrid double tube sections utilising seawater and sea sand concrete, FRP and stainless steel. *Thin-Walled Structures* 149: 106643.
Li YL, Teng JG, Zhao XL, et al. (2018a) Theoretical model for seawater and sea sand concrete-filled circular FRP tubular stub columns under axial compression. *Engineering Structures* 160: 71-84.
Li YL, Zhao XL, Raman Singh RK, et al. (2016) Experimental study on seawater and sea sand concrete filled GFRP and stainless steel tubular stub columns. *Thin-Walled Structures* 106: 390-406.
Li YL, Zhao XL and Singh Raman RK (2018b) Mechanical properties of seawater and sea sand concrete-filled FRP tubes in artificial seawater. *Construction and Building Materials* 191: 977-993.
Li YL, Zhao XL and Singh Raman RK (2019) Theoretical model for concrete-filled stainless steel circular stub columns under axial compression. *Journal of Constructional Steel Research* 157: 426-439.
Li YL, Zhao XL, Singh Raman RK, et al. (2018c) Thermal and mechanical properties of alkali-activated slag paste, mortar and concrete utilising seawater and sea sand. *Construction and Building Materials* 159: 704-724.
Li YL, Zhao XL, Singh Raman RK, et al. (2018d) Axial compression tests on seawater and sea sand concrete-filled double-skin stainless steel tubes. *Engineering Structures* 176: 426-438.
Litherland K, Oakley D and Proctor B (1981) The use of accelerated ageing procedures to predict the long term strength of GRC composites. *Cement and Concrete Research* 11(3): 455-466.
Liu H-K, Tai N-H and Lee W-H (2002) Effect of seawater on compressive strength of concrete cylinders reinforced by non-adhesive wound hybrid polymer composites. *Composites science and technology* 62(16): 2131-2141.
Liu T, Liu X and Feng P (2020) A comprehensive review on mechanical properties of pultruded FRP composites subjected to long-term environmental effects. *Composites Part B: Engineering*. 107958.
Liu W, Cui H, Dong Z, et al. (2016) Carbonation of concrete made with dredged marine sand and its effect on chloride binding. *Construction and Building Materials* 120: 1-9.
Mehta PK and Monteiro PJM (2006) *Concrete : microstructure, properties, and materials (3rd ed.)*. McGraw-Hill.
Micelli F and Myers J (2008) Durability of FRP-confined concrete. *Proceedings of the Institution of Civil Engineers-Construction Materials* 161(4): 173-185.
Mohammed TUT, Hamada H and Yamaji T (2004) Performance of seawater-mixed concrete in the tidal environment. *Cement and Concrete Research* 34(4): 593-601.
Mufti AA, Banthia N, Benmokrane B, et al. (2007) Durability of GFRP composite rods. *Concrete International* 29(02): 37-42.

Nishizaki I, Labossière P and Sarsaniuc B (2005) Durability of CFRP sheet reinforcement through exposure tests. *Special Publication* 230: 1419-1428.
Nkurunziza G, Debaiky A, Cousin P, et al. (2005) Durability of GFRP bars: A critical review of the literature. *Progress in Structural Engineering and Materials* 7(4): 194-209.
Raman R, Guo F, Al-Saadi S, et al. (2020) Understanding fibre-matrix degradation of FRP composites for advanced civil engineering applications: an overview. *Corrosion and Materials Degradation* 1(1): 27-41.
Ramaswamy S, Aziz M and Murthy C (1982) Sea dredged sand for concrete. *Extending Aggregate Resources*. ASTM International.
Sasaki I and Nishizaki I (2012) Tensile load relaxation of FRP cable system during long-term exposure tests. *Proceedings of the 6th international conference on FRP composites in civil engineering (CICE2012).*
Shalon R and Rapheal M (1959) Influence of sea water on corrosion of reinforcement. *Journal Proceedings.* 1251-1268.
Silva MA (2007) Aging of GFRP laminates and confinement of concrete columns. *Composite Structures* 79(1): 97-106.
Teng J-G, Xiang Y, Yu T, et al. (2019) Development and mechanical behaviour of ultra-high-performance seawater sea-sand concrete. *Advances in Structural Engineering* 22(14): 3100-3120.
Teng J, Yu T, Dai J, et al. (2011) FRP composites in new construction: current status and opportunities. *Proceedings of 7th National Conference on FRP Composites in Infrastructure (Supplementary Issue of Industrial Construction), keynote presentation.*
Teng JG, Huang YL, Lam L, et al. (2007) Theoretical model for fiber-reinforced polymer-confined concrete. *Journal of Composites for Construction* 11(2): 201-210.
Toutanji H and Balaguru P (1998) Durability characteristics of concrete columns wrapped with FRP tow sheets. *Journal of Materials in Civil Engineering* 10(1): 52-57.
Toutanji H and Deng Y (2002) Strength and durability performance of concrete axially loaded members confined with AFRP composite sheets. *Composites Part B: Engineering* 33(4): 255-261.
Wang S and ElGawady MA (2019) Durability of Hollow-Core GFRP–Concrete–Steel Columns under Severe Weather Conditions. *Journal of Composites for Construction* 23(1): 04018078.
Wang Z, Zhao X-L, Xian G, et al. (2017) Long-term durability of basalt-and glass-fibre reinforced polymer (BFRP/GFRP) bars in seawater and sea sand concrete environment. *Construction and Building Materials* 139: 467-489.
Wegian FM (2010) Effect of seawater for mixing and curing on structural concrete. *The IES Journal Part A: Civil & Structural Engineering* 3(4): 235-243.
Xiao J, Qiang C, Nanni A, et al. (2017) Use of sea-sand and seawater in concrete construction: Current status and future opportunities. *Construction and Building Materials* 155: 1101-1111.
Xie Z, Xie J, Guo Y, et al. (2018) Durability of CFRP-wrapped concrete exposed to hydrothermal environment. *International Journal of Civil Engineering* 16(5): 527-541.
Yamato T, Emoto Y and Soeda M (1987) Freezing and thawing resistance of concrete containing chloride. *Special Publication* 100: 901-918.
Yang S, Xu J, Zang C, et al. (2019) Mechanical properties of alkali-activated slag concrete mixed by seawater and sea sand. *Construction and Building Materials* 196: 395-410.
Younis A, Ebead U, Suraneni P, et al. (2018) Fresh and hardened properties of seawater-mixed concrete. *Construction and Building Materials* 190: 276-286.
Zeng J-J, Gao W-Y, Duan Z-J, et al. (2020) Axial compressive behavior of polyethylene terephthalate/carbon FRP-confined seawater sea-sand concrete in circular columns. *Construction and Building Materials* 234: 117383.